Neoplasma 2023; 70(3): 340–349

doi:10.4149/neo_2023_230110N17

NOP2-mediated m^{5}C methylation of XPD is associated with hepatocellular carcinoma progression

Guo-Fang SUN[1], Hao DING[2,*]

[1]Department of Electrocardiogram Diagnosis, The Second Affiliated Hospital of Nanchang University, Nanchang, Jiangxi, China; [2]Department of Gastroenterology, The Second Affiliated Hospital of Nanchang University, Nanchang, Jiangxi, China

**Correspondence: efydinghao1981@163.com*

Received January 10, 2023 / Accepted May 9, 2023

Hepatocellular carcinoma (HCC) is a common malignant tumor with high mortality. Our previous study has confirmed that XPD acts as an anti-oncogene and is downregulated in HCC. The mechanism of XPD downregulation in HCC is unclear. In this work, we obtained the datasets related to HCC patients from GSE76427, LIRI-JP, and TCGA-LIHC cohorts. Among 15 m^{5}C regulators (NSUN2, NSUN3, NSUN4, NSUN5, NSUN6, NSUN7, DNMT1, TRDMT1, DNMT3A, DNMT3B and NOP2, TET1, TET2, and TET3, ALYREF), 14 m^{5}C regulators were upregulated in tumor tissues of HCC patients, except for TET2. HCC patients were divided into Cluster A and B with different m^{5}C methylation patterns. Cluster B was enriched in metabolism-related signaling pathways, and Cluster A was prominently associated with the cell cycle signaling pathway. Moreover, XPD was positively correlated with NOP2. Cluster B exhibited upregulation of XPD and had an obvious survival advantage with respect to Cluster A. Additionally, NOP2 and XPD were downregulated in HCC tumors and cells. *In vitro* assays revealed that NOP2 overexpression enhanced XPD expression by elevating the m^{5}C methylation of XPD, which contributed to inhibit proliferation, migration, and invasion of HCC cells. In conclusion, this work demonstrated that XPD mRNA stability was elevated by NOP2-mediated m^{5}C methylation modification and then inhibited the malignant progression of HCC, suggesting that XPD may be a potential target for HCC treatment.

Key words: XPD; m5C methylation; NOP2; hepatocellular carcinoma

Liver cancer is a common cancer in the world, which is more prevalent in men [1]. About 90% of patients belong to hepatocellular carcinoma (HCC) [2]. Due to a deficiency of early symptoms and effective biomarkers, most patients are usually diagnosed in the late stage of the disease [3, 4]. Although the treatment of HCC has made significant progress with the development of medical technology and new drugs, about 70% of patients still have tumor recurrence and metastasis within five years after surgery [5]. Therefore, the goal and challenge of scientific research remain to study the pathogenesis of HCC and provide novel targets for its treatment.

Xeroderma pigmentosum gene D (XPD) is an important DNA repair gene, its gene product is the core component of mammalian basic transcription factor II H (TFIIH). It is widely involved in eukaryotic transcription initiation and the DNA nucleotide excision repair process [6]. XPD gene polymorphisms are risk factors for various cancers, including HCC [7–9]. Our previous study has found decreased expression of XPD in HCC tissues and cells. XPD overexpression represses malignant phenotypes of HCC cells and reduces the tumor formation of HCC [10]. Nevertheless, the underlying mechanism of the downregulation of XPD in HCC is still unclear.

RNA modification is dynamic, reversible, and widespread in different biological processes [11]. The mRNA cysteine is methylated when it undergoes a type of RNA modification called 5-methylcytosine (m^{5}C). It is mainly distributed in the CG enrichment region and depends on methyltransferases (writers), demethylases (erasers), and binding proteins (readers) [12]. m^{5}C methylation modification has a variety of biological functions, such as regulating mRNA transport, RNA stability, translation, and mitochondrial activity [12, 13]. It regulates various tumors' occurrence, development, invasion, and metastasis. For instance, higher expression of m^{5}C methylation-related genes NSUN3 and NSUN4 are observed in tumor tissues, and related to clinicopathological characteristics and survival rate of lung cancer [14].

The expression of m^5C methyltransferase NSUN2 is higher in bladder urothelial carcinoma than in normal tissues, thus promoting cancer development by enhancing the stability of oncogene HDGF [15]. Thus, we want to investigate whether XPD can participate in the progression of HCC through m^5C methylation modification.

This study integrated the genomic data from HCC samples and examined the m^5C modification patterns. Among the 15 m^5C regulators, NOP2 was positively correlated with XPD. *In vitro* assays demonstrated that NOP2 enhanced the stability of XPD and elevated the expression of XPD, thereby inhibiting malignant phenotypes of HCC cells.

Materials and methods

Data collection. The Cancer Genome Atlas (TCGA) provided the clinical data for liver hepatocellular carcinoma (LIHC), somatic mutation, copy number variation (CNV), and raw fragment per kilobase (FPKM) values. FPKM value was further converted into a transcript of one thousand base millions (TPM) value. The gene expression dataset and clinical trait data (the Liver Cancer-RIKEN JP) were collected from the ICGC database (https://dcc.icgc.org/). The GSE76427 dataset was downloaded from Gene Expression Omnibus (GEO) database (https://www.ncbi.nlm.nih.gov/gds/). Batch effects from non-biological technical biases were corrected using the "ComBat" algorithm of the sva package [16].

Unsupervised clustering of m^5C regulators. Based on the merged datasets from GSE76427, LIRI-JP, and TCGA-LIHC cohorts, 15 m^5C regulators were obtained, including 11 writers (NSUN2, NSUN3, NSUN4, NSUN5, NSUN6, NSUN7, DNMT1, TRDMT1, DNMT3A, DNMT3B, and NOP2), 3 readers (TET1, TET2, and TET3), 1 eraser (ALYREF). The expression of 15 m^5C regulators was used to identify distinct m^5C alteration patterns using unsupervised clustering analysis and to categorize patients. The consensus clustering algorithm was implemented by applying the ConsensuClusterPlus package to examine clusters and their stability [17].

Gene set variation analysis (GSVA) and functional annotation. "GSVA" R packages were utilized to examine the differences in biological processes in different m^5C modification patterns. The "c2. cp. kegg. v6.2. symbols" genome was obtained from the MsigDB database. It was considered statistically significant when the adjusted p-value <0.05. The "ClusterProfiler" R package was applied to annotate the m^5C-related genes under the threshold of error detection rate (FDR) <0.05.

Single sample gene set enrichment analysis (ssGSEA) of TME cell infiltration. ssGSEA algorithm was implemented to determine the enrichment fraction and relative abundance of cell infiltration in the tumor microenvironment (TME) of HCC. The gene sets related to invasive immune cells in TME were obtained from Charoentong, which stored information about various human immune cells [18, 19].

Participants. With the Ethics Committee of the Second Affiliated Hospital of Nanchang University's approval (No. Review [2022] No. 20), 19 HCC patients (the mean ± SD of age was 66.21±7.79) including 10 males and 9 females were enrolled in this study. There were 2 patients with stage I, 7 patients with stage II, 8 patients with stage III, and 2 patients with stage IV. Among them, 19 cases of tumor tissues and 17 cases of adjacent normal tissues were extracted from these HCC patients. Two cases of adjacent normal tissues were excluded. All participants provided informed consent. HCC tumor tissues were examined by surgical pathology. Before surgery, these patients had no other concomitant diseases and received no treatment, including chemotherapy or radiotherapy.

Cell culture and transfection. Human normal hepatocytes (LO2 cells) and HCC cell lines (HepG2, SMMC-7721, and Hep3B) were purchased from the Shanghai Institute of Biochemistry and Cell Biology (China). Cells were cultured in DMEM (Gibco, Grand Island, NY, USA) at 37 °C and 5% CO_2. It contained 10% fetal bovine serum (FBS; Gibco) and 1% penicillin/streptomycin.

Cell transfection. The vector pcDNA3.1 containing NOP2 (NOP2-OE) was constructed to induce NOP2 overexpression (Genepharm, Guangzhou, China). An empty vector (Vect) served as a control. SMMC-7721 cells were seeded into a 24-well plate at a density of 5×10^4 cells/plate. After 24 h of incubation, cells were transfected with 0.8 μg NOP2-OE or Vect applying 2 μl Lipofectamine 2000 Reagent (Thermo Fisher Scientific, Waltham, MA, USA). Cells were further cultured for 48 h and then collected for further analysis.

Quantitative real-time PCR (qRT-PCR). Total RNA was extracted from tissues and cells using the guidelines provided in the RNA isolation kit (Toyobo, Tokyo, Japan). Reverse transcription was carried out to synthesize cDNA using RevertAid RT Kit (Thermo Fisher Scientific). Then, an amplification reaction was carried out utilizing TB Green® Premix Ex Taq™ (Takara, Dalian, China) on the 7500 Real-time PCR system (Applied Biosystems, Foster City, CA, USA). The reaction mixture contained 10 μl TB Green Premix Ex Taq, 0.4 μl ROX Reference Dye II, 0.4 μl forward primer, 0.4 μl reverse primer, 2 μl DNA template, and 6.8 μl sterile water. The reaction mixture was incubated at 95 °C for 2 min, followed by 40 cycles at 95 °C for 30 s, 57 °C for 30 s and 72 °C for 30 s. The primer sequences (5'–3') of NOP2 and β-actin were displayed as follows: NOP2: forward-AAGGGTGCCGAGACAGAACT and reverse-GAGCACGACTAGACAGCCTC; XPD: forward-TCTGCCTCTGCCCTATGAT and reverse-CGATTCCCTCGGACACTTT; β-actin (loading control): forward-CTCGCCTTTGCCGATCC and reverse-TTCTCCATGTCGTCCCAGTT. The data were analyzed by the $2^{-\Delta\Delta Ct}$ method.

Methylated RNA immunoprecipitation (Me-RIP). Me-RIP was carried out to examine the m^5C methylation of XPD as a previous study described [20]. Briefly, SMMC-7721

cells were treated with RIP lysis buffer (Merck Millipore, Monmouth Junction, NJ, USA). Protein A/G magnetic beads were pre-treated with anti-m^{5}C (#ab10805, Abcam, Cambridge, MA, USA) or anti-IgG (#2729, Cell Signaling Technology, Danvers, MA, USA) for 2 h. Cells were incubated with antibody-beads complex with rotation at 4 °C. Subsequently, RNA was eluted from the beads and used to examine the enrichment of XPD by qRT-PCR.

Western blotting. Cells and tissues were treated with RIPA lysis buffer (Medchem Express), and total proteins were isolated from the cell and tissue lysate. The concentration of proteins was examined using BCA Protein Assay Kit (Beyotime, Shanghai, China). The proteins were separated by 10% SDS-PAGE gel electrophoresis and then transferred onto PVDF membranes. After blocking with 5% skimmed milk, the membranes were incubated with primary antibodies, anti-XPD (1:1000, #ab150362; Abcam), anti-NOP2 (1:1000, #ab271075; Abcam), anti-β-actin (1:2500, #ab8227; Abcam) at 4 °C overnight, and then stained with secondary antibody (1:10000, #ab6721; Abcam) at room temperature for 1 h. The bands were developed with BeyoECL Moon Kit (Beyotime) and then analyzed by ImageJ software.

MTT assay. SMMC-7721 cells (10,000) at the logarithmic phase were seeded into a 96-well plate and incubated at 37 °C for 48 h. Cells were stained with 10 μl MTT reagent (Beyotime) at 37 °C for 1 h, and then incubated with 100 μl Formazan for 3 h. Finally, Microplate Reader (Thermo Fisher Scientific) was applied to examine the absorbance value at 570 nm of each sample.

Colony formation assay. SMMC-7721 cell suspension at logarithmic phase was added into a 6-well plate (700 cells/well) and cultured at 37 °C for 2 weeks. The medium was changed every 3 days and the cell status was observed. Cell colonies were fixed with 4% paraformaldehyde for 30 min and stained with 1 ml 0.4% crystal violet for 20 min. Finally, the colony number was counted.

Wound healing. SMMC-7721 cells (1×10^5) were seeded into a 6-well plate and cultured until 90% of confluence. The cells were scratched using a sterilized toothpick and washed with PBS to remove the scratched cells. Cells were further cultured in FBS-free DMEM for 0 and 24 h. The scratch wound was observed under an optical microscope and analyzed by ImageJ software.

Transwell assay. 24-well Transwell chambers (Corning Incorporation, Corning, NY, USA) coated with Matrigel (BD Biosciences, Franklin Lakes, NJ, USA) were used for Transwell assays. SMMC-7721 cells (4×10^4) were seeded into the upper chamber, DMEM and 10% FBS were added into the lower chamber. After 48 h of invasion, the invading cells on the lower surface of the chamber were subjected to fixation and staining with 0.4% crystal violet. Cell invasion images were captured from five random fields and then quantified using ImageJ software.

Statistical analysis. Each assay was conducted three times. The data were analyzed using IBM SPSS 22.0 statistical software (Armonk, NY, USA). Data were presented as mean ± standard deviation. The statistical difference was examined using the one-way ANOVA method and the two-tailed Student's t-test. Kaplan Meier plotter was used to analyze the prognosis survival curve. Spearman analysis was used for correlation analysis. A p-value less than 0.05 was considered a significant difference.

Results

The landscape of genetic variation of m^{5}C regulators in HCC. The mutation incidence of 15 m^{5}C regulators was examined, including 11 writers, 1 eraser, and 3 readers, in HCC patients from the TCGA-LIHC cohort to identify the m^{5}C methylation modification in HCC. A total of 48 individuals had m^{5}C regulator mutations, with an incidence of 13.19%. TET2 had the highest mutation frequency, followed by that of TET1. No mutation was observed in NSUN5, NSUN6, and DNMT3B (Figure 1A). Further analysis of the CNV frequency of m^{5}C regulators showed that most m^{5}C regulators were enriched in copy number amplification. DNMT, NOP2, NSUN4, and TET2 exhibited an obvious frequency of CNV deletion (Figure 1B). Figure 1C revealed the CNV location of 15 m^{5}C regulators on chromosomes. Compared with normal tissues, all m^{5}C regulators were upregulated in tumor tissues of HCC patients, except for TET2 (Figure 1D).

Biological characteristics of two clusters with different m^{5}C methylation modification. Based on the GSE76427, LIRI-JP, and TCGA-LIHC cohorts, the consensus clustering algorithm (k=2) was used to produce two clusters with distinct m^{5}C methylation modifications, referred to as Cluster A and Cluster B (Supplementary Figures S1A, S1B). Furthermore, the risk/favorable factors of m^{5}C regulators are shown in Figure 2A. Except for NSNU6, all other m^{5}C regulators were the risk factors for HCC. NSNU6 was negatively correlated with NSNU4 and NSNU5. NOP2 was negatively correlated with ALYREF and NSUN6. Prognostic analysis for the two clusters uncovered that Cluster B had an obvious survival advantage with respect to Cluster A (Figure 2B). The evaluation of the expression of 15 m^{5}C regulators in two clusters revealed that with the exception of NOP2 and NSUN6, all m^{5}C regulators were substantially expressed in Cluster A. Interestingly, the expression of NOP2 and NSUN6 was increased in Cluster B (Figure 2C). GSVA enrichment analysis was carried out to test the biological behaviors between two clusters with distinct m^{5}C modification patterns. Cluster B was enriched in metabolism-related signaling pathways, such as retinol metabolism, fatty acid metabolism, tryptophan metabolism, and phenylalanine metabolism. Cluster A was prominently associated with the cell cycle signaling pathway (Figure 2D). Additionally, TME cell infiltration analysis demonstrated that the activated CD4 T cells and type 2 T helper cells were abundant in Cluster A. Cluster B was enriched in eosinophils, monocytes, plasmacy-

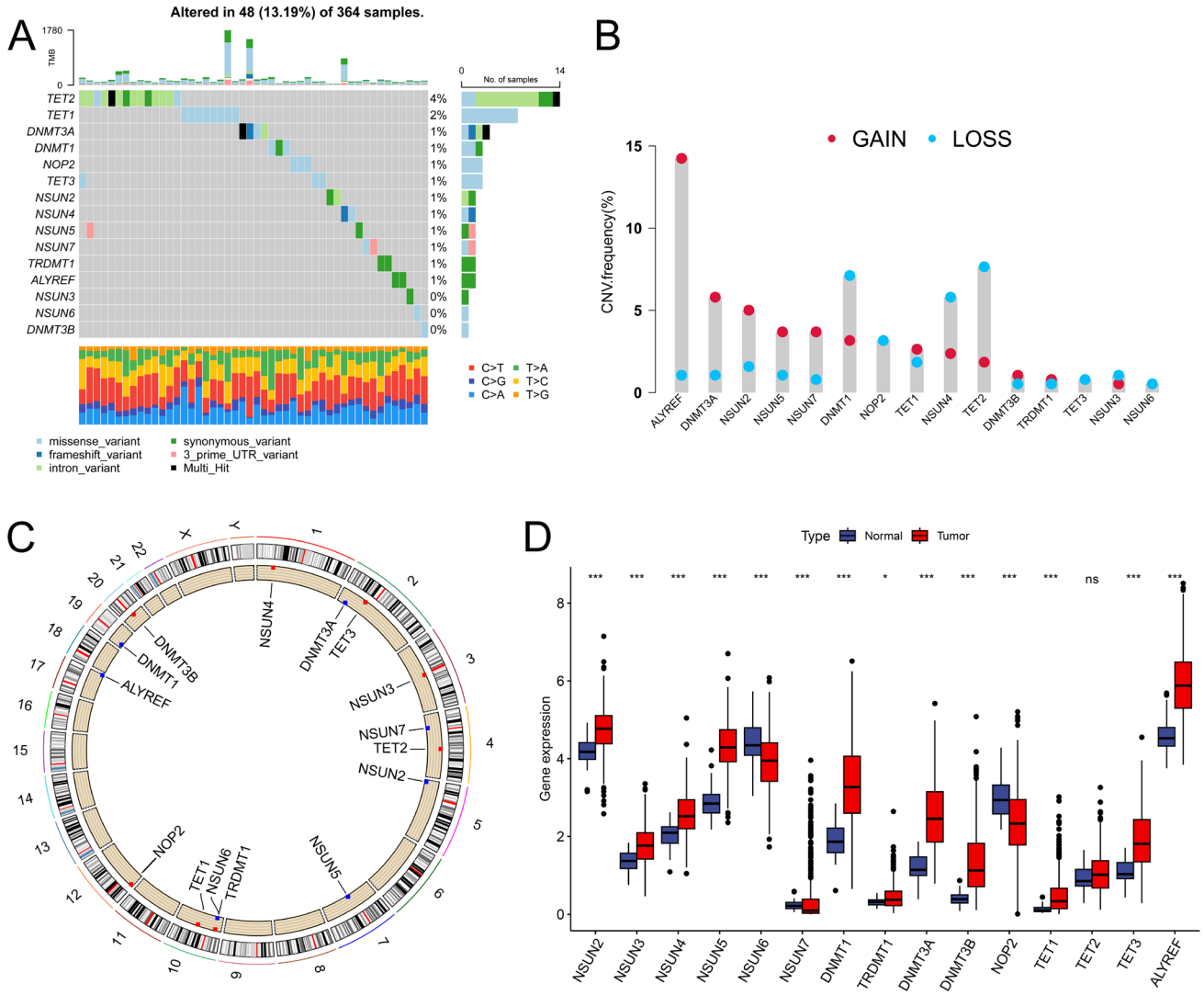

Figure 1. The landscape of genetic and expression variation of m^{5}C regulators in HCC. A) The mutation incidence of 15 m^{5}C regulators (11 writers, 1 eraser, and 3 readers) in HCC patients from the TCGA-LIHC cohort. B) The CNV variation frequency of m^{5}C regulators. C) The location of CNV alteration of m^{5}C regulators on 23 chromosomes. D) The expression of m^{5}C regulators between normal tissues and HCC tissues. *p<0.05, ***p<0.001; ns, not significant

toid dendritic cells, type 1 T helper cells, and type 17 T helper cells (Figure 2E).

The connection between NOP2/XPD expression and overall survival of HCC patients. The Spearman analysis of the correlations between the m^{5}C regulators and XPD in two clusters revealed that XPD had a positive correlation with NOP2 and a negative correlation with the other m^{5}C regulators (Figure 3A). Prognostic analysis for NOP2 and XPD expression revealed that compared with HCC patients with low expression of NOP2 and XPD, those with high expression of NOP2 and XPD usually indicated a better prognosis (Figures 3B, 3C). Interestingly, Cluster B had a higher expression of XPD than Cluster A (Figure 3D).

NOP2 and XPD were downregulated in HCC tissues and cells. The expression difference of NOP2 between 17 non-tumor and 19 HCC tumor tissues was quantified by qRT-PCR. Compared to non-tumor tissues, tumor tissues have significantly lower NOP2 and XPD mRNA expression (Figures 4A, 4C). NOP2 and XPD were discovered to be downregulated in tumor tissues using western blotting (Figures 4B, 4D). The same reduction of NOP2 and XPD mRNA and protein expression was also found in HCC cells (HepG2, SMMC-7721, and Hep3B) with respect to LO2 cells, as confirmed by qRT-PCR and western blotting (Figures 4E–4H). Thus, NOP2 and XPD may be closely associated with HCC development.

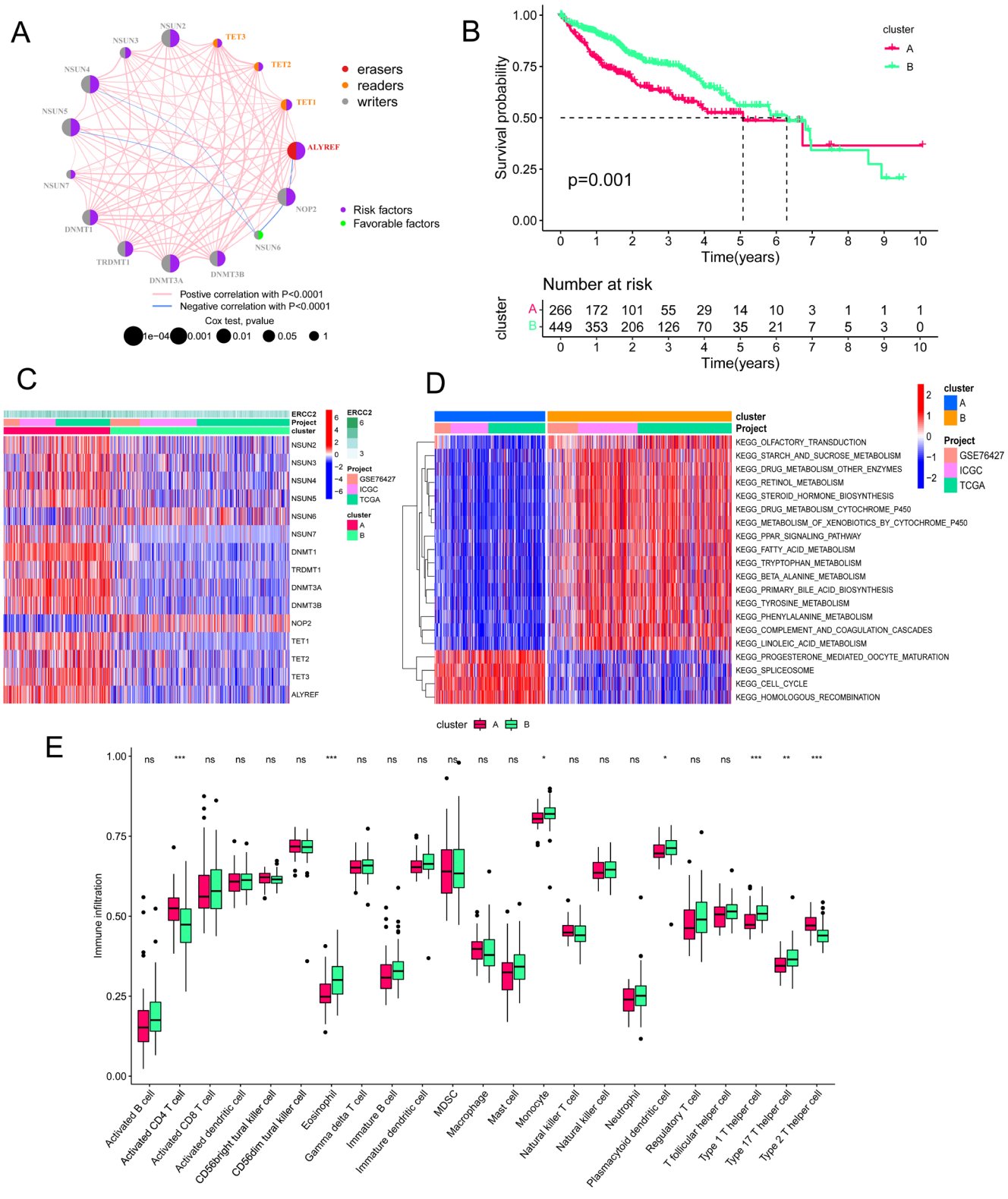

Figure 2. Biological characteristics of two clusters with different m^{5}C methylation modification. A) The interaction among 15 m^{5}C regulators in HCC. B) Kaplan-Meier curves analyzed the overall survival of HCC patients in Cluster A and B. C) Heatmap revealing the expression of m^{5}C regulators in Cluster A and B. D) GSVA enrichment analysis of the biological pathways in Cluster A and B. E) The abundance of each TME infiltrating cell in Cluster A and B. *p<0.05, **p<0.01, ***p<0.001; ns, not significant

NOP2 overexpression inhibited malignant phenotypes of HCC cells. NOP2 was overexpressed in SMMC-7721 cells to better understand how NOP2 affects the proliferation, migration, and invasion of HCC. Transfection of NOP2-OE effectively enhanced the expression of NOP2 protein (Figure 5A). This upregulation was accompanied by an increase in XPD mRNA and protein (Figures 5B, 5C). The cell proliferation ability of SMMC-7721 cells was examined by conducting MTT and colony formation assays. It was observed that the proliferation ability was notably reduced in NOP2-OE-expressing SMMC-7721 cells compared to Vect-transfected SMMC-7721 cells (Figures 5D, 5E). Applying wound healing and Transwell assays, reduction of migration and invasion was observed in SMMC-7721 cells following transfection of NOP2-OE (Figures 5F, 5G). MeRIP was used to determine how NOP2 affected the m^{5}C methylation of XPD, and the results showed that NOP2 overexpression in SMMC-7721 cells significantly increased the m^{5}C methylation of XPD (Figure 5H). All of these findings demonstrated that NOP2 overexpression caused SMMC-7721 cells to proliferate, migrate, and invade at a lower rate.

Discussion

In recent years, many studies have shown that the m^{5}C methylation modification is involved in regulating various tumors' occurrence, development, invasion, and metastasis. Here, the mutation and CNV variation of 15 m^{5}C regulators were observed in HCC patients. All m^{5}C regulators were upregulated in tumor tissues of HCC patients, except for

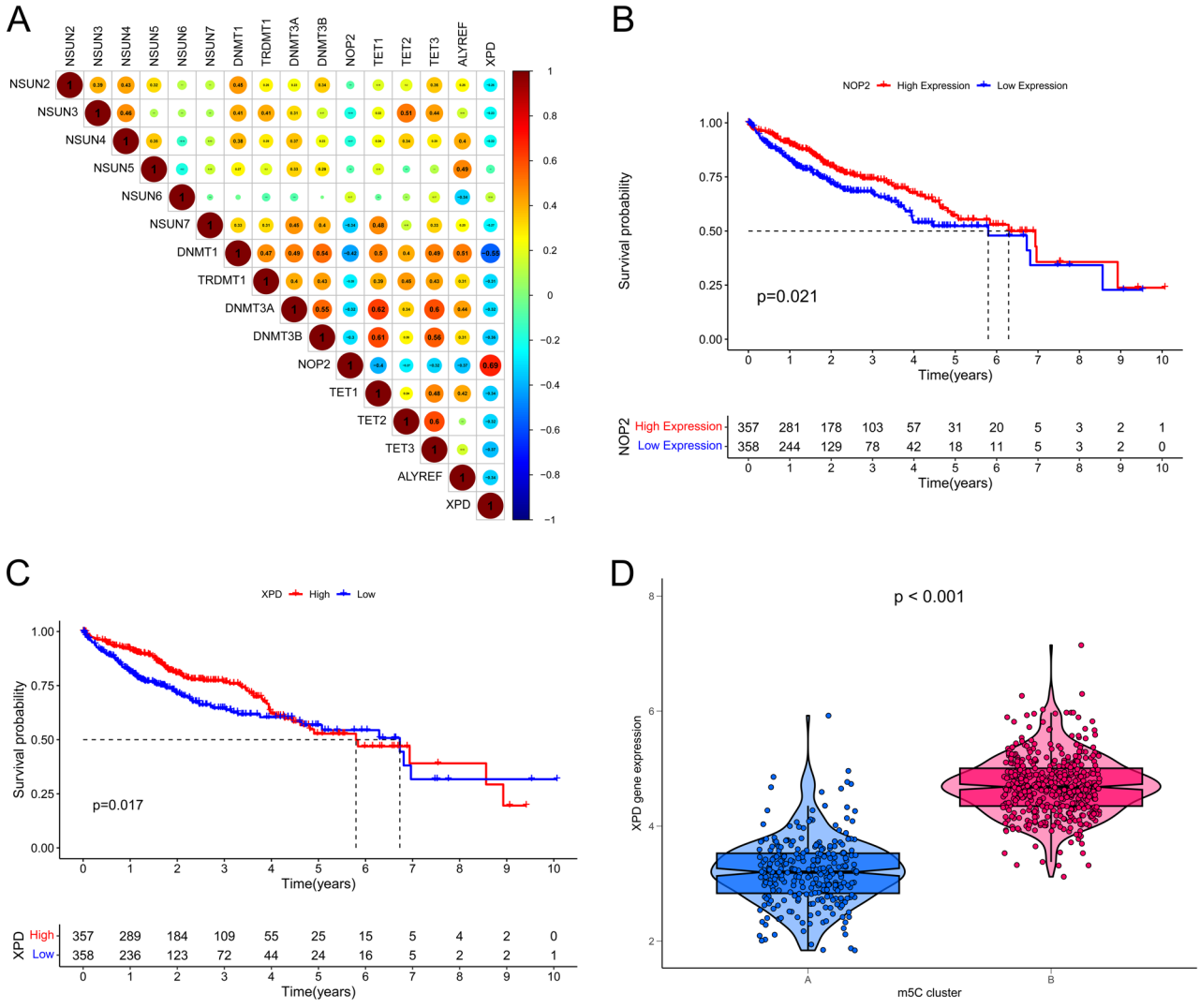

Figure 3. The connection between NOP2/XPD expression and overall survival of HCC patients. A) Correlations between 15 m^{5}C regulators and XPD in two clusters were evaluated by Spearman analysis. B, C) Kaplan-Meier curves analyzed the connection between NOP2/XPD expression and the overall survival of HCC patients in two clusters. D) The expression of XPD in Cluster A and B.

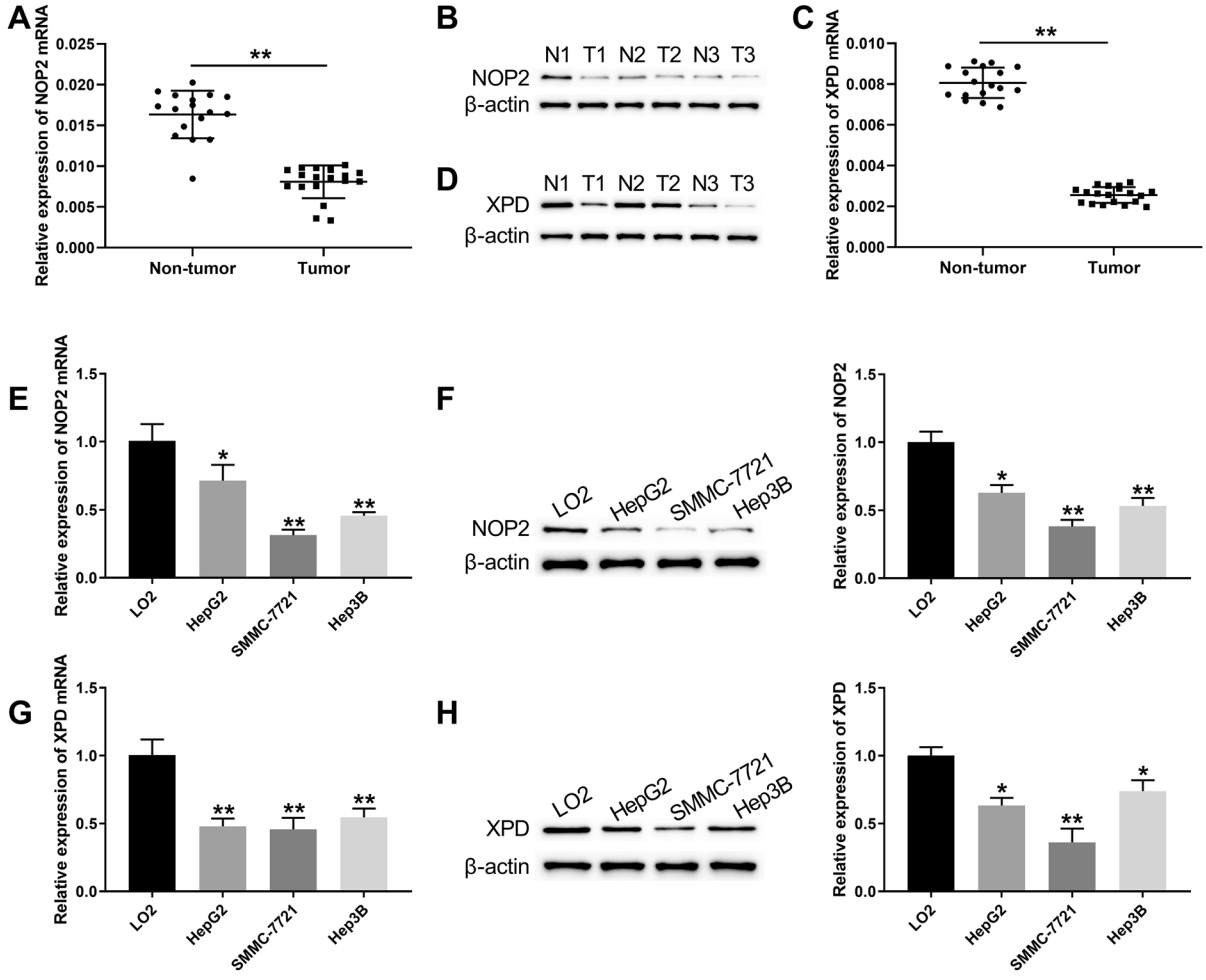

Figure 4. NOP2 and XPD were downregulated in HCC tumors and cells. qRT-PCR (A, C) and western blotting (B, D) examined NOP2 and XPD expression in tumor and non-tumor tissues of HCC patients. qRT-PCR (E, G) and western blotting (F, H) assessed NOP2 and XPD expression in LO2, HepG2, SMMC-7721, and Hep3B cells. *p<0.05, **p<0.01 non-tumor or LO2 group

TET2. Based on the expression of 15 m^5C regulators, HCC patients were divided into two clusters with different m^5C methylation patterns. Cluster B exhibited upregulation of NOP2 and NSUN6, and had an obvious survival advantage with respect to Cluster A. XPD was positively correlated with NOP2. Additionally, NOP2 and XPD were downregulated in HCC tumors and cells. NOP2 overexpression enhanced m^5C methylation of XPD to inhibit proliferation, migration, and invasion of HCC cells.

As one of the common epigenetic modifications in cancer, m^5C methylation regulates transcriptional activity [21]. The m^5C methylation is closely related to the occurrence, clinical diagnosis, prognosis, and treatment of various cancers. For instance, most m^5C modifications of miRNAs are observed in glioblastoma multiforme, and miRNA-181a-5p methylation modification is related to the poor prognosis of glioblastoma multiforme patients [22]. Based on 11 m^5C regulators, lung cancer samples are split into two m^5C methylation modification modes, each of which has a different level of immune cell infiltration in the TME [23]. Zhang et al. have carried out methylated RNA immunoprecipitation sequencing and found that the mRNA m^5C peak is widely distributed in tumor tissues of HCC patients as compared with adjacent tissues [23]. In HCC tumor tissues, both the frequency of circRNA and lncRNA m^5C methylation and the number of m^5C methylation genes are elevated [24, 25]. Here, HCC samples were divided into two clusters with different m^5C methylation patterns. Cluster B exhibited a better prognosis with respect to Cluster A. The activated CD4 T cells and type 2 T helper cells were abundant in Cluster A. Cluster B was enriched in eosinophils, monocytes, plasmacytoid dendritic cells, type 1 T helper cells, and type 17 T helper cells. Thus, m^5C methylation may regulate immune cell infiltration to affect TME in HCC.

NOP2 belongs to the NSUN gene family, which also includes six genes, NSUN2-7. The proteins encoded by

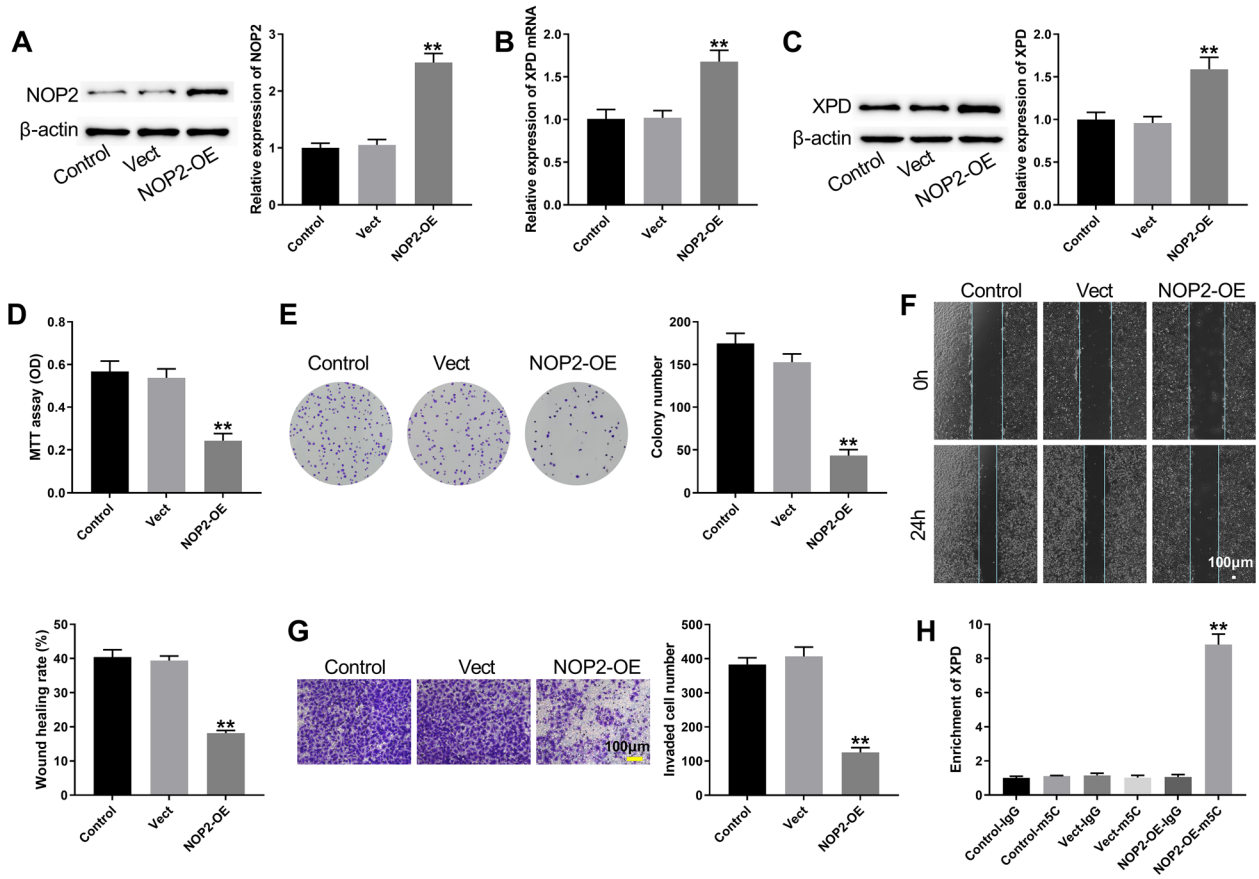

Figure 5. NOP2 overexpression enhanced m^{5}C methylation of XPD to inhibit malignant phenotypes of HCC cells. SMMC-7721 cells were transfected with NOP2-OE or Vector. A) Western blotting examined NOP2 expression in SMMC-7721 cells. qRT-PCR (B) and western blotting (C) detected XPD expression in SMMC-7721 cells. MTT assay (D) and clone formation assay (E) assessed the proliferation of SMMC-7721 cells. Wound healing assay (F) and Transwell assay (G) evaluated the migration and invasion of SMMC-7721 cells. H) Me-RIP assessed the m^{5}C methylation levels of XPD. **p<0.01 Vect group

these genes all have RNA methyltransferase activity and catalyze the formation of 5-methylcytosine modification from different kinds of RNA [12]. Additionally, the change of XPD polymorphism will directly affect the change of TFIIH complex activity, thereby causing abnormal DNA repair and transcription defects [26]. Thus, XPD polymorphisms play a vital role in tumorigenesis and development [27]. For instance, Gln/Gln variants of XPD increase smokers' lung cancer risk. Lys/Gln and Gln/Gln variants of XPD are strongly linked to lung cancer carcinogenesis in people with a family history of cancer [9]. A meta-analysis has confirmed that the polymorphisms of the XPD rs13181 G allele and rs1799793 T allele enhance the risk of HCC in the Chinese population [7]. Zhang et al. have found that XPD expression is decreased in HCC tumor tissues. XPD/miR-29a-3p axis negatively regulates COL4A1 expression to inhibit the malignant progression of HCC [28]. In the present work, we found that HCC patients with high expression of NOP2 had a better prognosis than HCC patients with low expression of NOP2. Moreover. the survival curve of patients with high and low expression of XPD after 4 years had overlapping parts, which cannot effectively distinguish the survival rate of patients. This may be due to the small sample size of patients who have survived for more than 4 years, resulting in the short survival time of patients with high expression of XPD at 50% survival rate. In addition, XPD may have a good distinction in the early stage of HCC. With the aggravation of tumor progression, the impact of XPD on the survival of HCC patients was no longer as effective as early differentiation of the survival rate of patients. Furthermore, the antitumor effect of XPD in HCC was confirmed. It was found that NOP2 and XPD were downregulated in HCC tumors and cells. NOP2 overexpression enhanced XPD expression to reduce proliferation, migration, and invasion of HCC cells. NOP2 may enhance the stability of XPD by promoting the m^{5}C methylation of XPD.

In summary, this work demonstrated that XPD mRNA stability was regulated by NOP2-mediated m^{5}C methylated modification, and then inhibited malignant progression of HCC, suggesting that XPD may be a potential target for HCC treatment.

Supplementary information is available in the online version of the paper.

Acknowledgments: This work was supported by the National Natural Science Foundation of China [grant number 82060443]; Natural Science Foundation of Jiangxi Province [grant number 20202BAB206050 and grant number 20202BABL206010]; Science and Technology Project of Health Commission of Jiangxi Province [grant number 202210620].

References

[1] SUNG H, FERLAY J, SIEGEL RL, LAVERSANNE M, SOERJOMATARAM I et al. Global Cancer Statistics 2020: GLOBOCAN Estimates of Incidence and Mortality Worldwide for 36 Cancers in 185 Countries. CA Cancer J Clin 2021; 71: 209–249. https://doi.org/10.3322/caac.21660

[2] FORNER A, REIG M, BRUIX J. Hepatocellular carcinoma. Lancet 2018; 391: 1301–1314. https://doi.org/10.1016/s0140-6736(18)30010-2

[3] EL-KHOUEIRY AB, SANGRO B, YAU T, CROCENZI TS, KUDO M et al. Nivolumab in patients with advanced hepatocellular carcinoma (CheckMate 040): an open-label, noncomparative, phase 1/2 dose escalation and expansion trial. Lancet 2017; 389: 2492–2502. https://doi.org/10.1016/s0140-6736(17)31046-2

[4] ISLAMI F, WARD EM, SUNG H, CRONIN KA, TANGKA FKL et al. Annual Report to the Nation on the Status of Cancer, Part 1: National Cancer Statistics. J Natl Cancer Inst 2021; 113: 1648–1669. https://doi.org/10.1093/jnci/djab131

[5] LASSANDRO G, PICCHI SG, BIANCO A, DI COSTANZO G, COPPOLA A et al. Effectiveness and safety in radiofrequency ablation of pulmonary metastases from HCC: a five years study. Med Oncol 2020; 37: 25. https://doi.org/10.1007/s12032-020-01352-2

[6] PEISSERT S, SAUER F, GRABARCZYK DB, BRAUN C, SANDER G et al. In TFIIH the Arch domain of XPD is mechanistically essential for transcription and DNA repair. Nat Commun 2020; 11: 1667. https://doi.org/10.1038/s41467-020-15241-9

[7] ZHOU Q, FU Y, WEN L, DENG Y, CHEN J et al. XPD Polymorphisms and Risk of Hepatocellular Carcinoma and Gastric Cancer: A Meta-Analysis. Technol Cancer Res Treat 2021; 20: 1533033821990046. https://doi.org/10.1177/1533033821990046

[8] XUE H, LU Y, LIN B, CHEN J, TANG F et al. The effect of XPD/ERCC2 polymorphisms on gastric cancer risk among different ethnicities: a systematic review and meta-analysis. PloS One 2012; 7: e43431. https://doi.org/10.1371/journal.pone.0043431

[9] NAIRUZ T, RAHMAN M, BUSHRA MU, KABIR Y. TP53 Arg72Pro and XPD Lys751Gln Gene Polymorphisms and Risk of Lung Cancer in Bangladeshi Patients. Asian Pac J Cancer Prev 2020; 21: 2091–2098. https://doi.org/10.31557/apjcp.2020.21.7.2091

[10] XIAO Z, WANG Y, DING H. XPD suppresses cell proliferation and migration via miR-29a-3p-Mdm2/PDGF-B axis in HCC. Cell Biosci 2019; 9: 6. https://doi.org/10.1186/s13578-018-0269-4

[11] JONKHOUT N, TRAN J, SMITH MA, SCHONROCK N, MATTICK JS et al. The RNA modification landscape in human disease. RNA 2017; 23: 1754–1769. https://doi.org/10.1261/rna.063503.117

[12] BOHNSACK KE, HÖBARTNER C, BOHNSACK MT. Eukaryotic 5-methylcytosine (m^5C) RNA Methyltransferases: Mechanisms, Cellular Functions, and Links to Disease. Genes (Basel) 2019; 10. https://doi.org/10.3390/genes10020102

[13] CHEN YS, YANG WL, ZHAO YL, YANG YG. Dynamic transcriptomic m(5) C and its regulatory role in RNA processing. Wiley interdisciplinary reviews. RNA 2021; 12: e1639. https://doi.org/10.1002/wrna.1639

[14] PAN J, HUANG Z, XU Y. m5C RNA Methylation Regulators Predict Prognosis and Regulate the Immune Microenvironment in Lung Squamous Cell Carcinoma. Front Oncol 2021; 11: 657466. https://doi.org/10.3389/fonc.2021.657466

[15] CHEN X, LI A, SUN BF, YANG Y, HAN YN et al. 5-methylcytosine promotes pathogenesis of bladder cancer through stabilizing mRNAs. Nat Cell Biol 2019; 21: 978–990. https://doi.org/10.1038/s41556-019-0361-y

[16] LEEK JT, JOHNSON WE, PARKER HS, JAFFE AE, STOREY JD. The sva package for removing batch effects and other unwanted variation in high-throughput experiments. Bioinformatics 2012; 28: 882–883. https://doi.org/10.1093/bioinformatics/bts034

[17] WILKERSON MD, HAYES DN. ConsensusClusterPlus: a class discovery tool with confidence assessments and item tracking. Bioinformatics 2010; 26: 1572–1573. https://doi.org/10.1093/bioinformatics/btq170

[18] CHAROENTONG P, FINOTELLO F, ANGELOVA M, MAYER C, EFREMOVA M et al. Pan-cancer Immunogenomic Analyses Reveal Genotype-Immunophenotype Relationships and Predictors of Response to Checkpoint Blockade. Cell reports 2017; 18: 248–262. https://doi.org/10.1016/j.celrep.2016.12.019

[19] BARBIE DA, TAMAYO P, BOEHM JS, KIM SY, MOODY SE et al. Systematic RNA interference reveals that oncogenic KRAS-driven cancers require TBK1. Nature 2009; 462: 108–12. https://doi.org/10.1038/nature08460

[20] YANG X, ZHANG S, HE C, XUE P, ZHANG L et al. METTL14 suppresses proliferation and metastasis of colorectal cancer by down-regulating oncogenic long non-coding RNA XIST. Mol Cancer 2020; 19: 46. https://doi.org/10.1186/s12943-020-1146-4

[21] HUANG T, CHEN W, LIU J, GU N, ZHANG R. Genome-wide identification of mRNA 5-methylcytosine in mammals. Nat Struct Mol Biol 2019; 26: 380–388. https://doi.org/10.1038/s41594-019-0218-x

[22] CHERAY M, ETCHEVERRY A, JACQUES C, PACAUD R, BOUGRAS-CARTRON G et al. Cytosine methylation of mature microRNAs inhibits their functions and is associated with poor prognosis in glioblastoma multiforme. Mol Cancer 2020; 19: 36. https://doi.org/10.1186/s12943-020-01155-z

[23] ZHANG Q, ZHENG Q, YU X, HE Y, GUO W. Overview of distinct 5-methylcytosine profiles of messenger RNA in human hepatocellular carcinoma and paired adjacent non-tumor tissues. J Transl Med 2020; 18: 245. https://doi.org/10.1186/s12967-020-02417-6

[24] HE Y, ZHANG Q, ZHENG Q, YU X, GUO W. Distinct 5-methylcytosine profiles of circular RNA in human hepatocellular carcinoma. Am J Transl Res 2020; 12: 5719–5729.

[25] HE Y, SHI Q, ZHANG Y, YUAN X, YU Z. Transcriptome-Wide 5-Methylcytosine Functional Profiling of Long Non-Coding RNA in Hepatocellular Carcinoma. Cancer Manag Res 2020; 12: 6877–6885. https://doi.org/10.2147/cmar.S262450

[26] COIN F, BERGMANN E, TREMEAU-BRAVARD A, EGLY JM. Mutations in XPB and XPD helicases found in xeroderma pigmentosum patients impair the transcription function of TFIIH. EMBO J 1999; 18: 1357–1366. https://doi.org/10.1093/emboj/18.5.1357

[27] CLARKSON SG, WOOD RD. Polymorphisms in the human XPD (ERCC2) gene, DNA repair capacity and cancer susceptibility: an appraisal. DNA repair 2005; 4: 1068–1074. https://doi.org/10.1016/j.dnarep.2005.07.001

[28] ZHANG H, WANG Y, DING H. COL4A1, negatively regulated by XPD and miR-29a-3p, promotes cell proliferation, migration, invasion and epithelial-mesenchymal transition in liver cancer cells. Clin Transl Oncol 2021; 23: 2078–2089. https://doi.org/10.1007/s12094-021-02611-y

https://doi.org/10.4149/neo_2023_230110N17

NOP2-mediated m^{5}C methylation of XPD is associated with hepatocellular carcinoma progression

Guo-Fang SUN[1], Hao DING[2,*]

Supplementary Information

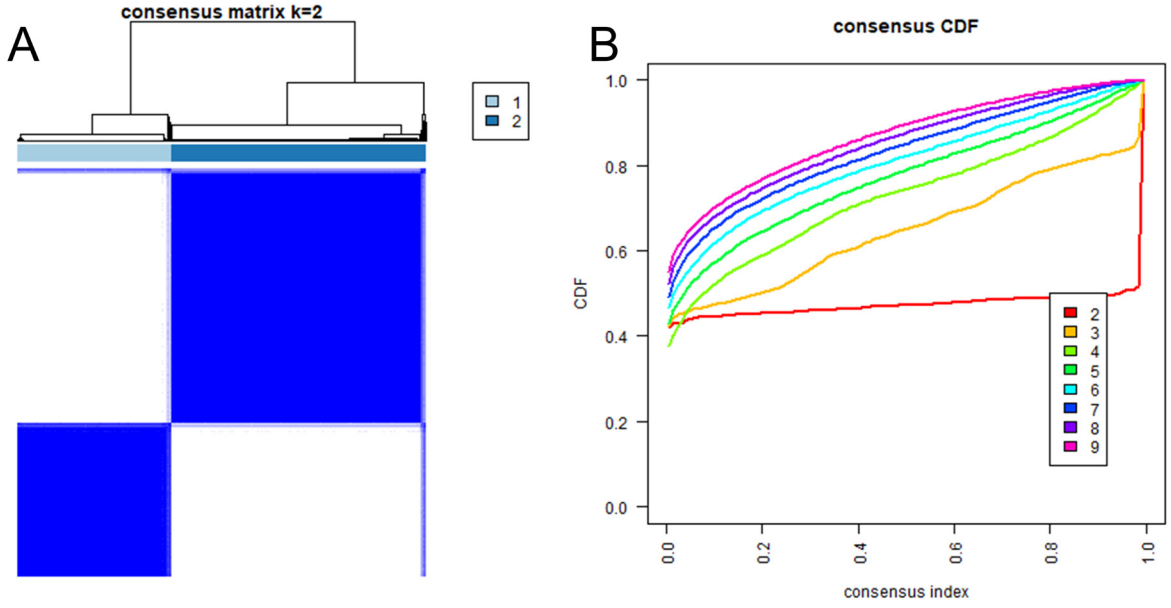

Supplementary Figure S1. Two clusters of HCC patients with different m5C methylated modification. A) Two clusters with different m5C methylated modification were divided by consensus clustering algorithm (k=2) based on GSE76427, LIRI-JP and TCGA-LIHC cohort. B) Cumulative distribution function (CDF) curves with different "k" values.